

CHAPTER 15

NATURE'S STRATEGY FOR OXIDIZING TRYPTOPHAN: EPR AND MÖSSBAUER CHARACTERIZATION OF THE UNUSUAL HIGH-VALENT HEME Fe INTERMEDIATES

KEDNERLIN DORNEVIL AND AIMIN LIU

Department of Chemistry, Georgia State University, Atlanta, GA, USA

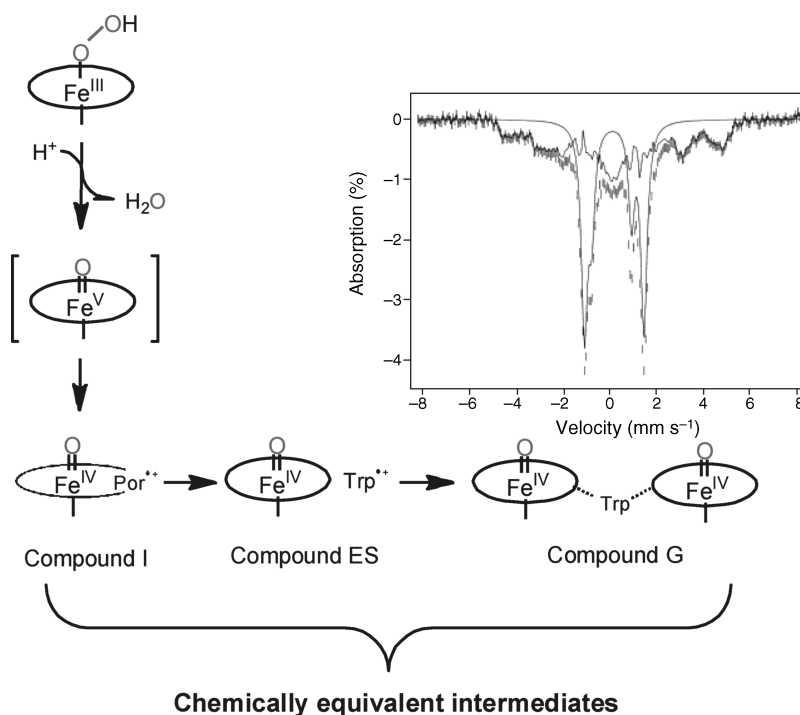
15.1 TWO OXIDIZING EQUIVALENTS STORED AT A FERRIC HEME

Heme (iron protoporphyrin IX) proteins play important roles in a wide array of biological functions, including single-electron transfer mediation, oxygen transport and storage, redox reactions, detoxification, and transcription regulation. Heme proteins are also known to play a key role in many metabolic processes involving oxidation reactions to satisfy the needs required for sustaining life. Redox reactions involve the transfer of electrons to and from a heme and thus produce heme intermediates with distinct oxidation states of the iron ion, some of ~~are~~ which are high-valent Fe intermediates. The term “high valent” is defined here as the iron ion with an oxidation state exceeding III. The most common heme Fe oxidation states found in biological chemical reactions are the ferrous, ferric, and ferryl species [1–4]. Mössbauer spectroscopy, which can detect and characterize Fe species in all forms, is thus an indispensable tool for understanding the fundamental aspects of heme chemistry in enzymology. In the past decades, the high-valent Fe chemistry developed from biochemical, spectroscopic, and modeling studies has provided key insights into numerous essential biological processes that involve enzymes with Fe cofactors [5]. Thus, the importance of high-valent Fe intermediates in heme and nonheme systems has become widely appreciated.

Since the oxidation or oxygenation reactions involving molecular oxygen are generally two- or four-electron processes, an important piece of chemistry is to understand how the metal centers store and stabilize the oxidizing equivalents. When two oxidizing equivalents are stored at a heme center, the most common form of the heme intermediate is known as compound I (cpd I), which is a classical intermediate with a ferryl ion, that is, Fe(IV)=O , coupled with a π -cation radical located on the porphyrin ring (Por) (Fig. 15.1). Such a heme Fe intermediate transiently stabilizes two oxidizing equivalents above the resting Fe(III), and is chemically equivalent to an Fe(V) species. Until now, Fe(V) intermediates have not yet been observed in any biological reaction. Compound I appears to be the most popular natural evolution of the strategy for storing

FIGURE 15.1

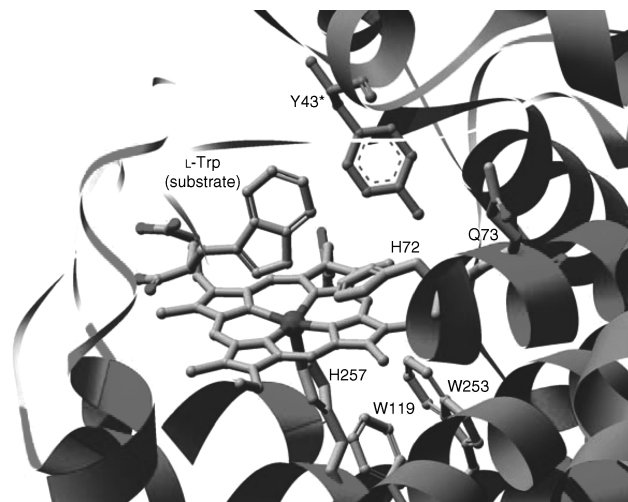
Nature's strategies to store two oxidizing equivalents in heme proteins. The inset shows a Mössbauer spectrum of a bis-Fe(IV) intermediate in MauG [7]. The hashed marks are the experimental data of diferric MauG reacting with 1 equiv of H_2O_2 for 45 s. The noisy line indicates the contribution of ferric heme ($\sim 34\%$ of total Fe). The simulated smooth solid line represents two Fe(IV) species. See the text for details.



oxidizing power on a heme moiety. Similar to an Fe(V) species, the two oxidizing equivalents in cpd I are stored in the heme cofactor. However, cpd I is a much more manipulable system than Fe(V) due to its higher chemical stability gained from the charge distribution to the porphyrin ring. This is a great advantage for promoting biological reactions because the organic substrates need to bind to the enzyme active site and orientate properly. At the same time, the enzyme active site often needs reorganization and conformational changes in order to activate substrates or stabilize transient intermediates. The oxidative heme intermediate should not be too reactive to accommodate the required substrate orientation and active site reorganization. Another common form of the high-valent Fe species in heme proteins is compound ES (cpd ES), which is composed of an Fe(IV)=O heme and amino acid-based cation radical in close proximity to the high-valent heme. The compound ES description is based on the initial characterization from cytochrome *c* peroxidase (CCP) [6]. In cytochrome *c* peroxidase, compound ES is derived from the transfer of the porphyrin cation radical of a compound I-type intermediate to a nearby tryptophan (Trp) residue. Likewise, cpd ES is also an intermediate state with two oxidizing equivalents above the original ferric state. In the following, we will review the discovery of a third high-valent Fe heme intermediate termed compound G (cpd G), which carries the two oxidizing equivalents in two discrete hemes and presents a bis-Fe(IV) intermediate (Fig. 15.1). Cpd G is an unprecedented Fe species. This intermediate was found from a diheme enzyme that oxidizes tryptophan residues in the substrate protein. The spatial separation of the two oxidizing equivalents found in cpd G results in unique consequences in stability and chemical properties of the intermediate. This chapter will review its discovery and discuss its biological and general chemical significance.

15.2 OXIDATION OF L-TRYPTOPHAN BY HEME-BASED ENZYMES

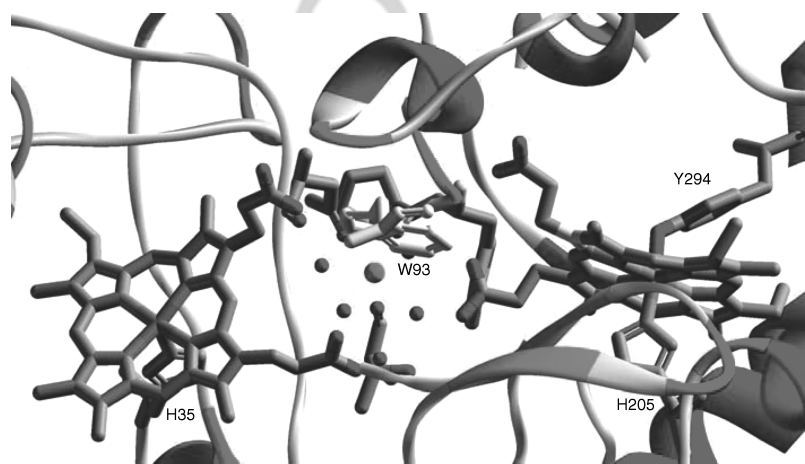
L-Tryptophan is an essential amino acid for humans. The majority of the dietary supply of Trp is metabolized in the kynurenine pathway in which tryptophan 2,3-dioxygenase (TDO), the enzyme that converts Trp to *N*-formylkynurenine (NFK), catalyzes the first and committed step. In addition to being an important metabolite, Trp is also involved in various biochemical activities. When cross-linked and oxygenated, two Trp residues can serve as cofactors for amine oxidations in several enzymes [8,9]. Furthermore, Trp plays many indirect biologically significant roles. In the kynurenine pathway, several metabolites generated from Trp oxidation are known to display neuroactive properties [10,11]. Kynurenic acid is a neuroprotectant and endogenous antagonist at *N*-methyl-D-aspartic acid (NMDA) receptors, while quinolinic acid is an agonist of these receptors. L-Tryptophan is also an endogenous source of NAD production, and the kynurenine pathway

**FIGURE 15.2**

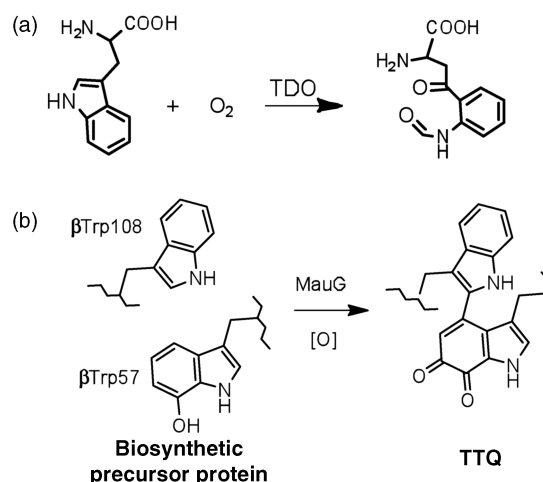
The ligand-bound structure of tryptophan 2,3-dioxygenase (PDB: 2NW7). (See the color version of this figure in Color Plates section.)

constitutes the major part of the *de novo* biosynthetic route of NAD [10–12]. The oxidation of the amino acid tryptophan is thus an important biological event.

Recent reports have linked the oxidation/oxygenation of free and protein-bound Trp to heme-based proteins, that is, TDO (Fig. 15.2) and MauG (Fig. 15.3), respectively. The oxidation of free Trp is carried out by TDO, which inserts two oxygen atoms into Trp in a four-electron oxidizing process by utilizing a *b*-type heme cofactor (Fig. 15.4a). This enzyme is representative of a potentially new hemoprotein dioxygenase superfamily whose oxygenase mechanism remains poorly understood. It should be noted that dioxygenase activity is typically accomplished by nonheme metalloenzymes. The nonheme iron active sites generally have two histidines, one carboxylate, and two or three solvent-derived metal ligands, which allow simultaneous binding of both substrate and dioxygen by replacing the solvent-derived labile ligands. The primary substrate and O₂ bind to a nonheme metal ion and thus both become activated. The metal ion functions as a conduit so that the electrons of the primary substrate move to O₂ through the metal ion. In some cases, such as α -ketoglutarate-dependent dioxygenases, a cosubstrate is needed for production of an oxygenated intermediate followed by attack of the primary substrate. In contrast, the heme cofactor does not allow binding of the primary substrate and O₂ because porphyrin and the proximal ligand are not labile. In TDO, after binding of O₂ the heme Fe becomes coordination saturated; therefore, the primary substrate must bind to a pocket adjacent to the Fe ion [13]. Thus, the Fe ion cannot function as a bridge in between the primary substrate and O₂. The oxygen activation and insertion of TDO must proceed with a distinct mechanism relative to the well-characterized nonheme Fe-dependent dioxygenase enzymes. The oxidation of protein-bound Trp residues is catalyzed by a novel enzyme MauG, which utilizes two *c*-type hemes to catalyze a posttranslational modification of a 119 kDa protein and is an example of an enzyme that oxidizes protein-bound tryptophan residues. The reaction is a six-electron oxidation, and the utilization of two *c*-type hemes by MauG to perform the hydroxylation and subsequent oxidation reactions is unprecedented (Fig. 15.3).

**FIGURE 15.3**

The structure of the di-heme cofactor in MauG (PDB code: 3L4M). (See the color version of this figure in Color Plates section.)

**FIGURE 15.4**

The chemical reactions catalyzed by TDO (a) and MauG (b), respectively.

15.3 THE CHEMICAL REACTION CATALYZED BY MauG

While TDO oxidizes free Trp in a fast reaction, MauG oxidizes specific tryptophan residues within a large protein in a relatively slower catalytic process [14]. In methylamine dehydrogenase (MADH) from *Paracoccus denitrificans*, the catalytic center is a tryptophan tryptophylquinone (TTQ) cofactor, present on each β subunit of the 119 kDa heterotetrameric $\alpha_2\beta_2$ protein [15,16]. The TTQ cofactor is derived from Trp57 and Trp108 in a posttranslational process. The biogenesis of TTQ requires incorporation of two oxygen atoms into Trp57 and cross-linking of the indole rings of Trp57 and Trp108 of the β subunits (Fig. 15.4b) [17]. Such a biosynthesis is, however, not a self-processing event but an enzyme-mediated posttranslational process that requires the action of at least one processing enzyme encoded in the methylamine utilization (*mau*) gene cluster [18,19]. It has been shown that MauG, the 42.3 kDa *mauG* gene product, is the crucial enzyme for TTQ biogenesis [20,21]. MauG catalyzes the second oxygenation (at C6 of the Trp57 phenyl ring), the cross-linking of the two tryptophan residues (Trp57 and Trp108), and the oxidation of the semiquinone intermediate during the TTQ biogenesis [22]. Deletion of *mauG* in the *mau* gene cluster causes an accumulation of a 119 kDa biosynthetic precursor of MADH in which Trp57 is monohydroxylated at C7 and the cross-link is absent [23]. This 119 kDa protein precursor of MADH is the natural substrate of MauG. The TTQ biosynthesis from the precursor is achievable *in vitro* using either O_2 plus electrons from an external donor or H_2O_2 .

MauG is the first enzyme described that utilizes *c*-type hemes to carry out oxygenase activity (Fig. 15.3). This enzyme exhibits sequence homology to bacterial diheme cytochrome *c* peroxidase, but it possesses negligible peroxidase activity [21]. The initial characterization of MauG by EPR spectroscopy suggests that this diheme enzyme is similar to heme-based oxygenase enzymes such as heme oxygenase (HO) and P450 with bound inhibitors [21]. Subsequent biochemical and mass spectrometry studies establish that MauG performs an unusual six-electron oxidation reaction, presumably two per step in three successive steps, to insert an oxygen atom into a Trp residue on the substrate protein and remove four protons from the oxygenated Trp and another adjacent Trp residue to produce a cross-linked TTQ cofactor on the substrate protein (Fig. 15.4b). Such a quinone cofactor is the catalytic center for MADH. The MauG-mediated reaction is essentially the terminal step of the MADH cofactor biogenesis.

The unique utilization of two *c*-type hemes to perform oxygenation and subsequent oxidation reactions contrasts other hemoproteins that generally utilize *b*-type hemes, such as P450 [5,24,25], for their oxygenase activity. Most recently, a few other enzymes have also been found to utilize *c*-type hemes to perform similar reactions. For instance, RoxA is a rubber oxygenase that utilizes two *c*-type hemes for an oxidative cleavage of poly(*cis*-1,4-isoprene) [26]. As the best characterized protein in this potential new group of hemoproteins, MauG is an ideal model for studying the catalytic mechanisms of those covalently bound *c*-type heme cofactors. Another special aspect of MauG is that its substrate is a pair of protein-bound tryptophan residues inside a protein, which is about threefold larger in size than the enzyme itself. The characterization of MauG-catalyzed TTQ biosynthesis is carried out with the expectation to expand the existing knowledge about protein evolution, protein structure–function relationships, and protein engineering strategies for introducing new functional groups into proteins.

Sequence alignment, biochemical, and EPR study of MauG reveals that the two ferric hemes are present in a distinct spin state [21]. The high-spin ferric heme is ligated with a histidine (His35) ligand. The low-spin ferric heme is six-coordinate with two protein ligands, one of which is His205 [21]. The two His ligands, one for each heme, are confirmed to provide the proximal axial heme ligands by the X-ray structural study of the enzyme [27]. The EPR and intrinsic oxidation–reduction midpoint potential studies of MauG reveal a redox cooperativity, that is, facile equilibration of electrons, between the two hemes [28,29]. However, EPR studies show that the two hemes are not spin coupled [7,21]. Therefore, the two hemes must be distantly located even though they efficiently share electrons. The physical separation of the two hemes was later verified by the crystal structure of the enzyme in complex with its substrate protein at 2.1 Å resolution [27]. The two Fe ions are ~ 21 Å apart although the heme edges are within 10 Å of each other and are connected through H-bonds by Trp93 [27]. A recent spectroscopic study also shows that the His–Tyr ligation remains unchanged at the fully reduced diferrrous state [29]. At both the diferrrous and diferric oxidation states, only the five-coordinate heme reacts with exogenous molecules such as O_2 and nitric oxide (NO). The six-coordinate heme does not directly react with exogenous molecules. The distal Tyr ligand appears to remain bound to the heme during the chemical reaction of the five-coordinate heme [29].

15.4 A HIGH-VALENT BIS-Fe(IV) INTERMEDIATE IN MauG

Upon mixing MauG with stoichiometric amounts of H_2O_2 , a new intermediate is formed. This species is stable and is characterized in UV–Vis by a Soret peak shift from 405 to 407 nm. The X-band EPR spectrum of MauG displays two heme signals, a high-spin signal ($g = 5.57, 1.99$) and a low-spin signal ($g = 2.54, 2.19, 1.87$). After mixing with H_2O_2 , both high- and low-spin signals disappear and a new radical signal can be observed at $g = 2.003$ with a peak-to-peak width of 1.3 mT [7]. The EPR characterization of the $g = 2.003$ radical suggests that it is an organic free radical. However, quantitation from spin double integration is that the radical signal represents 1% of the protein and cannot compensate for the loss of the two ferric heme EPR signals.

When ^{57}Fe -labeled MauG is treated with H_2O_2 , the resultant Mössbauer spectra show two sharp lines (intermediate) and an additional broad, magnetically split feature associated with ferric heme [7]. Upon subtraction of the ferric species, the resulting spectrum is fitted by two quadrupole doublets with the following parameters: isomer shift (δ_1) of 0.06 mm s^{-1} and quadrupole splitting parameter (ΔE_{Q1}) of 1.70 mm s^{-1} , and $\delta_2 = 0.17 \text{ mm s}^{-1}$ and $\Delta E_{Q2} = 2.54 \text{ mm s}^{-1}$ (Fig. 15.1, inset). The isomer shift values are typical of Fe(IV) [30] species and the quadrupole splitting parameter of species 1 is in the range typically observed for ferryl and protonated ferryl species [31]. The quadrupole splitting parameter of species 2 is unusually large ($\Delta E_{Q2} = 2.54 \text{ mm s}^{-1}$) and is likely due to the proposed six-coordinate heme with two axial amino acid ligands. The detailed spectral characterization of this intermediate is reported in Ref. 7. A recent quantum chemical study found that the unusual Mössbauer properties of both Fe(IV) species originated from novel structural features of the enzyme [32].

To our knowledge, the spin-uncoupled bis-Fe(IV) species found in MauG is an unprecedented Fe intermediate that represents a novel natural strategy to oxidize a large substrate (Fig. 15.5). We therefore named it cpd G. This species is analogous to the bis-ligated high-valent inorganic porphyrin model compounds that were generated previously. In all such cases, only a small isomer shift (δ) and a large quadruple splitting (ΔE_Q) parameter were observed from those model compounds [33,34]. Compound G also contains a six-coordinate Fe(IV) heme species with two axial amino acid ligands in

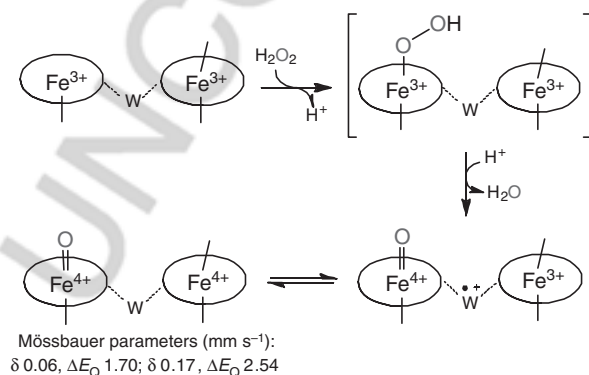


FIGURE 15.5

The reaction of diferric MauG with 1 equiv of hydrogen peroxide generates a catalytic bis-Fe(IV) intermediate [7].

protein. In the previous Fe(IV) intermediates characterized, an exogenous oxygen is attached to the Fe(IV) ion as an oxo ligand to effectively stabilize the high-valent charge. In contrast, this role is fulfilled by the distal Tyr ligand and a Trp residue rests in between the two hemes.

15.5 A HIGH-VALENT Fe INTERMEDIATE OF TRYPTOPHAN 2,3-DIOXYGENASE

While hemoproteins perform a wide range of biological functions, they rarely express a dioxygenase activity as the native biological function. TDO is the first enzyme known to utilize a heme cofactor to express dioxygenase activity [35]. TDO catalyzes the oxidative cleavage of the indole ring of L-tryptophan, converting it to NFK in the absence of a coenzyme or an external electron donor (Fig. 15.4a). This activity is the initiating and the committing step for Trp to enter into the kynurenine pathway [12]. In mammals, TDO is responsible for oxidizing over 99% of the free Trp in intracellular and extracellular pools of this amino acid; hence, it is a biologically significant enzyme [10]. TDO is a tetramer composed of identical subunits with a total mass of 134 kDa. Each subunit contains a *b*-type heme cofactor. However, the four heme cofactors display two types of spectroscopic properties upon substrate binding despite the α_4 subunit structure [36]. The discovery of the inequivalent hemes in the enzyme–substrate complex is consistent with the cooperative binding of substrate [37].

The high-valent Fe(IV) intermediate of TDO has been proposed in computational studies but has not yet been directly observed in the catalytic cycle [38]. However, such a high-valent Fe(IV) heme has been observed by stopped-flow resonance Raman spectroscopy in its sister enzyme, indoleamine 2,3-dioxygenase (IDO) [39]. IDO and TDO are evolutionally related enzymes that catalyze the same chemical reaction. IDO is a monomeric protein existing in all human tissues except the liver. The lack of substrate binding cooperativity in IDO results in a slower chemical reaction and thus affords a great opportunity to directly trap the reactive intermediates. The IDO Fe(IV)=O intermediate is shown to display a characteristic 799 cm^{-1} for $\nu_{\text{Fe}=\text{O}}$ stretching mode with histidine as a proximal ligand of the heme [39].

Although a similar Fe(IV)=O intermediate of IDO has not yet been directly observed in the catalytic cycle of TDO, it has been trapped and characterized in the enzyme reactivation study. The ferric form of TDO can be reactivated by H_2O_2 in the presence of Trp through a complex mechanism [40]. When Fe(III)-TDO reacts with H_2O_2 in the absence of Trp, the Fe ion becomes EPR-silent and a protein-based radical is observed (Fig. 15.6). The free radical decays over time, while the EPR signal of the high-spin ferric heme restores. The ferric ion is shown by Mössbauer spectroscopy to

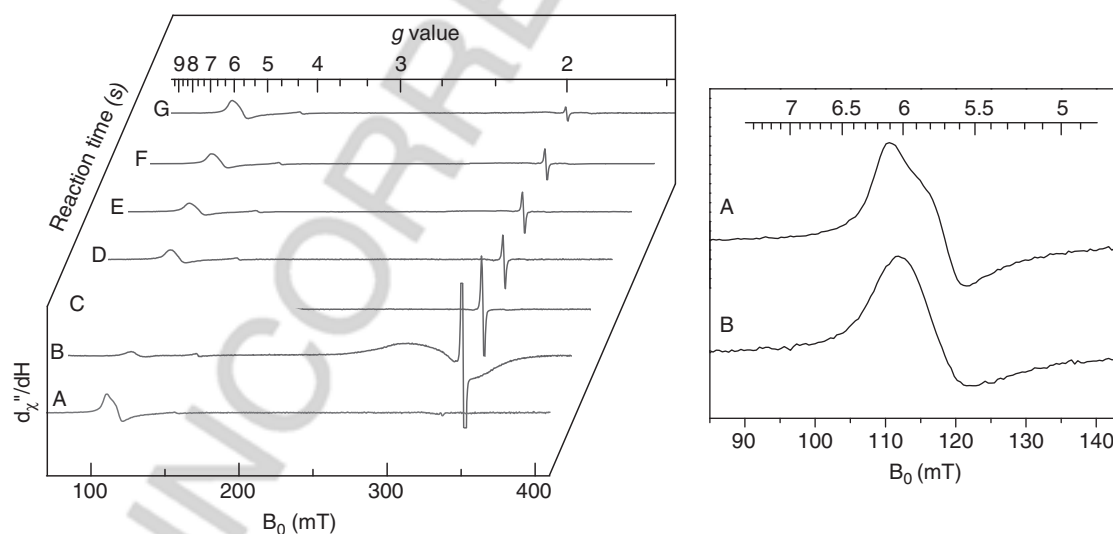


FIGURE 15.6

The formation and decay of the compound I-type ferryl intermediate in the reaction of $150\ \mu\text{M}$ tryptophan 2,3-dioxygenase with $900\ \mu\text{M}$ hydrogen peroxide monitored by EPR spectroscopy at 10 K. (a) Seven representative EPR spectra (traces A to G) are shown in a 2D plot for the reaction of 0, 12, 30, 60, 90, 240, and 600 s in the parallel samples. (b) The high spin EPR signal of TDO (A), H_2O_2 treated TDO at 30 s (B).

TABLE 15.1 Mössbauer Parameters of Selected Heme-Based Fe(IV)=O Species

Intermediate	Iron Species	<i>trans</i> Ligand	Spin	δ (mm s ⁻¹)	ΔE_Q (mm s ⁻¹)
TDO [40]	Fe ⁴⁺ =O ₂ ⁻	Histidine	S = 1	0.055	1.755
MauG [7]	Fe ⁴⁺ =O ₂ ⁻	Histidine	S = 1	0.06	1.70
HRP-I [41]	Fe ⁴⁺ =O ₂ ⁻	Histidine	S = 1	0.08(1)	1.25(1)
HRP-II [42]	Fe ⁴⁺ =O ₂ ⁻	Histidine	S = 1	0.03	1.61
CPO-II [31]	Fe ⁴⁺ =O ₂ ⁻	Cysteine	S = 1	0.11(3)	1.59(5)
CCP [6]	Fe ⁴⁺ =O ₂ ⁻	Histidine	S = 1	0.05	1.55
Catalase II [43]	Fe ⁴⁺ =O ₂ ⁻	Tyrosine	S = 1	0.07(2)	1.47(2)
CPO-I [44]	Fe ⁴⁺ =O ₂ ⁻	Cysteine	S = 1	0.15	1.02

become a ferryl intermediate [40]. The Mössbauer parameters of the Fe(IV)=O intermediate are nearly identical to those found for the Fe(IV)=O heme in cpd G (Table 15.1). The similar Fe(IV)=O intermediates exhibited by two structurally diverse heme containing enzymes are intriguing. Given the similarity of the catalytic function of the two enzymes, that is, oxidizing either free or protein-bound tryptophan, the striking similarity in the key intermediates is not very surprising.

The proposed protonated state of heme-based ferryl species has been studied in systems such as chloroperoxidase (CPO), cytochrome c peroxidase, cytochrome P450, catalase, horseradish peroxidase (HRP), and myoglobin (Mb) and is still under investigation [4]. Indeed, both cysteine and tyrosine (donating anionic ligands) are able to stabilize multiple forms of a ferryl species. In both cases, the equilibrium between the two seems to favor the deprotonated forms at physiologically relevant pH [31,43]. In addition, the presented histidine-ligated ferryls have a quadrupole splitting, the value of which is far less than the anticipated value for a protonated ferryl species (>2 mm s⁻¹) [45]. Thus, if the values of the quadrupole splitting parameter of TDO and MauG do represent protonated species, then there must be other contributing factors that can lower the value for these intermediates. Due to the nature of the reaction, it is possible that these enzymes are using secondary ligands to fine-tune the properties of the high-valent Fe intermediates. This can already be seen in the DFT calculations that predicted hydrogen bonding interactions from secondary ligands in the enzyme active site [32].

15.6 CONCLUDING REMARKS

The molecular biochemistry exhibited by two structurally diverse heme-containing enzymes that oxidize either free or protein-bound tryptophan residues is fascinating. Mono- and bis-Fe(IV) intermediates have been trapped and characterized by EPR and Mössbauer spectroscopy from these enzymes [7,40]. In particular, the bis-Fe(IV) intermediate (cpd G) found in MauG is unprecedented. The target Trp residues of substrate are remotely located from the hemes, ~40 Å from the heme that reacts with exogenous molecules. Thus, a long-range remote catalysis must take place in MauG. Recently, the cocrystal structure of MauG and its substrate protein preMADH has been reported. When the crystal is soaked in a solution containing H₂O₂, the TTQ product is formed in the substrate protein [27]. Thus, the proposed long-range remote catalysis is validated [46]. It should be noted that one of the indelible stories about spatial separation of the catalytic center and the site that stores oxidizing equivalent(s) is described in ribonucleotide reductase [47]. In that case, the catalytic center is located in the R1 subunit, while the oxidizing power, a protein-bound Tyr radical, is generated and stabilized by a metal center in the R2 subunit. When the substrate is loaded properly in the active site of R1 subunit, a long-range radical transfer takes place and a thiol-based transient radical is generated at the expense of the Tyr radical for the nucleotide reduction. The chemistry found in MauG is much like that found in ribonucleotide reductase and is more straightforward in terms of the nature of remote catalysis [46]. The diheme cofactor in MauG reacts with exogenous oxidants, generates high-valent Fe intermediate, and then transmits oxidizing equivalents to the substrate protein. Unquestionably, cpd G or bis-Fe(IV) is a new natural strategy discovered thus far for harnessing the problem of substrates way too large for an enzyme to accommodate. In this case, a remote catalysis must take place. Thus, the unprecedented bis-Fe(IV) intermediate found in MauG occupies an entry position for future study of long-range remote catalysis by metalloenzymes.

REFERENCES

1. H. Fujii, *Coord. Chem. Rev.* **2002**, *226*, 51–60.
2. D.L. Harris, *Curr. Opin. Chem. Biol.* **2001**, *5*, 724–735.
3. Y. Watanabe, High-valent intermediates, in *Porphyrin Handbook*, K.M. Kadish, K.M. Smith, R. Guilard, eds., Vol. 4, Academic Press, New York, **2000**, pp. 97–117.
4. A. Gumiero, C.L. Metcalfe, A.R. Pearson, E.L. Raven, P.C.E. Moody, *J. Biol. Chem.* **2011**, *286*, 1260–1268.
5. M. Sono, M.P. Roach, E.D. Coulter, J.H. Dawson, *Chem. Rev.* **1996**, *96*, 2841–2888.
6. G. Lang, K. Spartalian, T. Yonetani, *Biochim. Biophys. Acta* **1976**, *451*, 250–258.
7. X. Li, R. Fu, S. Lee, C. Krebs, V.L. Davidson, A. Liu, *Proc. Natl. Acad. Sci. USA* **2008**, *105*, 8597–8600.
8. W.S. McIntire, D.E. Wemmer, A. Chistoserdov, M.E. Lidstrom, *Science* **1991**, *252*, 817–824.
9. N.M. Okeley, W.A. van der Donk, *Chem. Biol.* **2000**, *7*, R159–R171.
10. T.W. Stone, L.G. Darlington, *Nat. Rev. Drug Discov.* **2002**, *1*, 609–620.
11. R. Schwarcz, *Curr. Opin. Pharmacol.* **2004**, *4*, 12–17.
12. O. Kurnasov, V. Goral, K. Colabroy, S. Gerdes, S. Anantha, A. Osterman, T.P. Begley, *Chem. Biol.* **2003**, *10*, 1195–1204.
13. F. Forouhar, J.L. Anderson, C.G. Mowat, S.M. Vorobiev, A. Hussain, M. Abashidze, C. Bruckmann, S.J. Thackray, J. Seetharaman, T. Tucker, R. Xiao, L.C. Ma, L. Zhao, T.B. Acton, G.T. Montelione, S.K. Chapman, L. Tong, *Proc. Natl. Acad. Sci. USA* **2007**, *104*, 473–478.
14. S. Lee, S. Shin, X. Li, V.L. Davidson, *Biochemistry* **2009**, *48*, 2442–2447.
15. L. Chen, R.C. Durley, F.S. Mathews, V.L. Davidson, *Science* **1994**, *264*, 86–90.
16. L. Chen, M. Doi, R.C. Durley, A.Y. Chistoserdov, M.E. Lidstrom, V.L. Davidson, F.S. Mathews, *J. Mol. Biol.* **1998**, *276*, 131–149.
17. Y. Wang, X. Li, L.H. Jones, A.R. Pearson, C.M. Wilmot, V.L. Davidson, *J. Am. Chem. Soc.* **2005**, *127*, 8258–8259.
18. C.J. van der Palen, D.J. Slotboom, L. Jongejan, W.N. Reijnders, N. Harms, J.A. Duine, R.J. van Spanning, *Eur. J. Biochem.* **1995**, *230*, 860–871.
19. M.E. Graichen, L.H. Jones, B.V. Sharma, R.J. van Spanning, J.P. Hosler, V.L. Davidson, *J. Bacteriol.* **1999**, *181*, 4216–4222.
20. A.R. Pearson, S. Marimanikkuppam, X. Li, V.L. Davidson, C.M. Wilmot, *J. Am. Chem. Soc.* **2006**, *128*, 12416–12417.
21. Y. Wang, M.E. Graichen, A. Liu, A.R. Pearson, C.M. Wilmot, V.L. Davidson, *Biochemistry* **2003**, *42*, 7318–7325.
22. X. Li, L.H. Jones, A.R. Pearson, C.M. Wilmot, V.L. Davidson, *Biochemistry* **2006**, *45*, 13276–13283.
23. A.R. Pearson, T. De La Mora-Rey, M.E. Graichen, Y. Wang, L.H. Jones, S. Marimanikkuppam, S.A. Agger, P.A. Grimsrud, V.L. Davidson, C.M. Wilmot, *Biochemistry* **2004**, *43*, 5494–5502.
24. P.R. Ortiz de Montellano, *Cytochrome P450: Structure, Mechanism, and Biochemistry*, 2nd edn, Plenum Press, New York, **1995**.
25. J.E. Erman, L.P. Hager, S.G. Sligar, *Adv. Inorg. Biochem.* **1994**, *10*, 71–118.
26. R. Braaz, W. Armbruster, D. Jendrosseck, *Appl. Environ. Microbiol.* **2005**, *71*, 2473–2478.
27. L.M.R. Jensen, R. Sanishvili, V.L. Davidson, C.M. Wilmot, *Science* **2010**, *327*, 1392–1394.
28. X. Li, M. Feng, Y. Wang, H. Tachikawa, V.L. Davidson, *Biochemistry* **2006**, *45*, 821–828.
29. R. Fu, F. Liu, V.L. Davidson, A. Liu, *Biochemistry* **2009**, *48*, 11603–11605.
30. P.G. Debrunner, Mössbauer spectroscopy of Fe porphyrins, in *Iron Porphyrins, Physical Bioinorganic Chemistry Series*, Vol. 4, A.B.P. Lever, H.B. Gray, eds., VCH Publishers, Inc., New York, **1989**, pp. 137–234.
31. K.L. Stone, L.M. Hoffart, R.K. Behan, C. Krebs, M.T. Green, *J. Am. Chem. Soc.* **2006**, *128*, 6147–6153.
32. Y. Ling, V.L. Davidson, Y. Zhang, *J. Phys. Chem. Lett.* **2010**, *1*, 2936–2939.
33. J.T. Groves, R. Quinn, T.J. McMurry, M. Nakamura, G. Lang, B. Boso, *J. Am. Chem. Soc.* **1985**, *107*, 354–360.
34. E. Bill, V. Schunemann, A.X. Trautwein, R. Weiss, J. Fischer, A. Tabard, R. Guilard, *Inorg. Chim. Acta* **2002**, *339*, 420–426.
35. Y. Kotake, I. Masayama, *Z. Physiol. Chem.* **1936**, *243*, 237–244.
36. R. Gupta, R. Fu, A. Liu, M.P. Hendrich, *J. Am. Chem. Soc.* **2010**, *132*, 1098–1109.
37. E. Fukumura, H. Sugimoto, Y. Misumi, T. Ogura, Y. Shiro, *J. Biochem.* **2009**, *145*, 505–515.
38. L.W. Chung, X. Li, H. Sugimoto, Y. Shiro, K. Morokuma, *J. Am. Chem. Soc.* **2010**, *132*, 11993–12005.
39. A. Lewis-Ballester, D. Batabyal, T. Egawa, C. Lu, Y. Lin, M.A. Marti, L. Capece, D.A. Estrin, S.-R. Yeh, *Proc. Natl. Acad. Sci. USA* **2009**, *106*, 17371–17376.
- Q3 40. R. Fu, R. Gupta, S. Wang, J. Geng, K. Dornevil, Y. Zhang, M.P. Hendrich, A. Liu, *J. Am. Chem. Soc.* **2011**, in press.
41. C.E. Schulz, R. Rutter, J.T. Sage, P.G. Debrunner, L.P. Hager, *Biochemistry* **1984**, *23*, 4743–4754.

REFERENCES

323

42. T. Harami, Y. Maeda, Y. Morita, A. Trautwein, U. Gonser, *J. Chem. Phys.* **1977**, *67*, 1164–1169.
43. O. Horner, J.L. Oddou, J.M. Mouesca, H.M. Jouve, *J. Inorg. Biochem.* **2006**, *100*, 477–479.
44. R. Rutter, L.P. Hager, H. Dhonau, M. Hendrich, M. Valentine, P. Debrunner, *Biochemistry* **1984**, *23*, 6809–6816.
45. R.K. Behan, M.T. Green, *J. Inorg. Biochem.* **2006**, *100*, 448–459.
46. J.M. Bollinger Jr., M.L. Matthews, *Science* **2010**, *327*, 1337–1338.
47. J. Stubbe, D.G. Nocera, C.S. Yee, M.C.Y. Chang, *Chem. Rev.* **2003**, *103*, 2167–2201.

UNCORRECTED PROOF

Author Query

1. References are arranged sequentially. Please check for correctness.
2. Please check the suggested citation of Fig. 15.5 in the text for correctness.
3. Please update Ref. 40.

UNCORRECTED PROOF